

Stability analysis of Shapiro steps in Josephson-junction arrays

H. Eikmans and J.E. van Himbergen

Institute for Theoretical Physics, University of Utrecht, P.O. Box 80.006, 3508 TA Utrecht, The Netherlands

(Received 13 March 1991)

The coupled set of evolution equations of the individual resistively shunted junctions in an array is written in a form that directly reveals the existence of a single-junction solution (SJS) for specific values of the external magnetic field. We formulate a condition that determines these field strengths in terms of the corresponding ground-state configurations. By studying the linearized evolution equations, around this coherent-phase solution, we show that the array is phase locked to the external source when the SJS is stable. Only in this case does it have relevance in practice. Our analysis clearly indicates that there are only regular Shapiro steps in the regions of stability, and in between these regions our simulations confirm the absence of fractional steps, reported earlier. Furthermore, simulations, also in fields with no SJS, demonstrate a degree of insensitivity to the field strength, which is only partly understood.

I. INTRODUCTION

Recent experiments¹ in arrays of tunnel junctions driven by a radio frequency (rf) source

$$I_{\text{ext}}(t) = I_{\text{dc}} + I_{\text{ac}} \sin(2\pi\nu_0 t), \quad (1.1)$$

have revealed steps in the time-averaged voltage, $\langle V \rangle$, across the array as a function of I_{dc} . The arrays consist of a rectangular lattice with superconducting islands, each of which is linked to its nearest neighbors by Josephson junctions, and the rf current is applied in the [01] direction. On a Shapiro step the value of $\langle V \rangle$, calculated per junction in the current direction, can be written as $(n/q)h\nu_0/(2e)$, for integers n and q . The steps clearly reflect the occurrence of collective phase locking of the junctions in the array to the external source. Particularly striking is the appearance of steps in the $I_{\text{dc}}-\langle V \rangle$ characteristic at integer values of $q > 1$. These measurements were explained using the intuitive picture of rigid vortex lattice motion.^{1,2}

In the arrays the magnetic field is usually measured as the flux f piercing a unit cell of the array in units of the elementary flux quantum $\phi_0 = hc/(2e)$. It is easy to see that the behavior of an array is periodic in f with period 1, and is invariant under $f \rightarrow -f$, so that one only needs to consider the interval $0 \leq f \leq \frac{1}{2}$. When a magnetic field is applied, automatically, each unit cell contains a vortex charge equal to f . The interaction between vortices is logarithmic at large intervortex distances. A consequence of the long range of the interaction is that the system will try to make the total vortex charge in the array equal to zero. To this end vortices with a charge -1 are induced in a fraction f of the cells, and these vortices are mobile. When an external current is applied, such a vortex experiences a Lorentz-like force, perpendicular to the current.³

For specific values of f , the density of mobile vortices are such that they can form a lattice which is commensurate with the underlying physical lattice. Phase locking at values of $\langle V \rangle$ with $q > 1$ occurs when such a vortex lattice moves rigidly over a number of unit cells of

the physical lattice. This picture is in agreement with observations^{2,4} in dynamic simulations.

In single junctions the regular steps, occurring at $q = 1$, are characterized by a trajectory in phase space which is periodic in time with the period $\tau_0 = 1/\nu_0$. Here, the $q > 1$ steps can only⁵ occur for underdamped junctions (for a review see, e.g., Refs. 6 and 7). These steps are then referred to as subharmonics and the trajectory in phase space does not have the τ_0 periodicity. In this sense the $q > 1$ steps in the single junctions are fundamentally different from the $q = 1$ steps in a single junction and also from the $q > 1$ steps in the arrays. The existence of anomalous steps in a simulation of arrays was reported at $f = \frac{1}{5}$.² Enabled by a very effective method,⁸ we have extensively simulated arrays with realistic (free) boundaries, and established absence of such steps in these systems.

The physical consequences of the aforementioned commensurability are manifest in various quantities, like, e.g., the array's magnetoresistance⁸⁻¹⁰ and critical current.⁹⁻¹³ In large arrays the effects are most pronounced at fractional values with a small denominator, like $f = \frac{1}{2}, \frac{1}{3}$, etc.; however, in smaller systems this need not be true. Both experiment and simulation show that in ladder arrays the major effects occur at other values if one replaces the usual geometry by a staircase geometry pictured in Fig. 1.⁸

The studies of the Shapiro steps mentioned above all consider an array in the form of a rectangular lattice. Given the critical importance of geometric features for the magnetoresistance, an interesting question remains with respect to the influence on the steps of the array geometry. Recently, Sohn *et al.* also studied the Shapiro steps in staircase arrays, and Halsey introduced a theoretical approach of the phenomenon in such arrays. The experiments and simulations¹⁴ show that there are only $q = 1$ steps, a result at variance with the proposed theory,¹⁵ which predicts subharmonic steps. The results in Ref. 14 were plausibly explained from the simulations, which reveal that the voltage differences over all the junctions in the array are equal at all times. Therefore, the

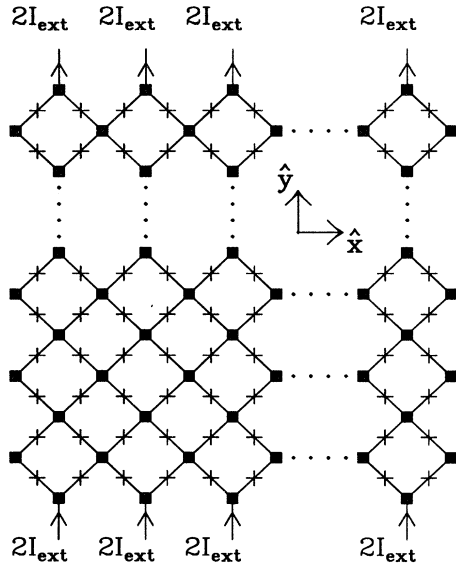


FIG. 1. Array with a staircase geometry. Each column has a current source of its own. With this convention the array carries its critical current when I_{ext} is equal to the junctions critical current I_c (i.e., when $i_{\text{ext}} = 1$). Crosses represent junctions; squares represent islands.

discrepancy between theory and (computer) experiment becomes even more puzzling.

It is the purpose of this work to gain more complete insight in this behavior. We find that the key to full understanding lies in a stability analysis of the full single-junction-type solution. Instead of deducing the correct equation for the coherent-phase part of the solution from the results of the simulation, we rewrite the full set of equations in a form that enables us to find not only the solution itself, but also the exact preconditions for existence. Next we explain the step width on the basis of stability of the coherent phase solution, and find that the mechanism through which this solution loses stability gives rise to an intrinsic rounding of the curve near the steps. Moreover, we demonstrate how an *ad hoc* assumption, made to ensure stability, actually leads the theory to give the spurious subharmonic steps. By showing explicitly how the stability analysis can actually be performed with respect to the continuous phase variables, one sees that this assumption is in fact an unnecessary artifact, leading to steps that are indeed not seen. Our simulation results for several values of f , in both finite and periodic arrays, show a large degree of insensitivity of the behavior of the arrays to changes in the magnetic field, which is only partly understood. Finally the scheme presented here for the practical analysis of the stability of solutions of the dynamic equations, may prove useful in other situations.

II. THE SINGLE-JUNCTION SOLUTION

We consider arrays of N junctions with a geometry as pictured in Fig. 1. The external current is of the

form given by Eq. (1.1), but measured in units of I_c it is denoted by $i_{\text{ext}}(t)$. In the present context it is natural to give the voltage difference in units of $\hbar\nu_0/(2e)$ and the resulting dimensionless quantity, averaged over all junctions in the array and over time is $\langle v \rangle$. The unit of time is given by $\hbar/(2eI_cR_n)$, where R_n is the normal state resistance of the individual junctions. The resistively shunted junction model is employed to solve the single-junction dynamics. For the junction occupying bond $\langle \mathbf{r}, \mathbf{r}' \rangle$ and carrying a total current $i(\mathbf{r}, \mathbf{r}', t)$ this leads to

$$\dot{\varphi}(\mathbf{r}, t) - \dot{\varphi}(\mathbf{r}', t) = i(\mathbf{r}, \mathbf{r}', t) - \sin[\varphi(\mathbf{r}, t) - \varphi(\mathbf{r}', t) - 2\pi A(\mathbf{r}, \mathbf{r}')], \quad (2.1)$$

where

$$A(\mathbf{r}, \mathbf{r}') = \frac{1}{\phi_0} \int_{\mathbf{r}}^{\mathbf{r}'} \mathbf{A}(\mathbf{r}, \mathbf{r}') \cdot d\mathbf{l}. \quad (2.2)$$

Here, the $\varphi(\mathbf{r}, t)$ represents the phase of the superconducting island at position \mathbf{r} . The vector potential is denoted by \mathbf{A} , and the previously introduced f equals the sum of the $A(\mathbf{r}, \mathbf{r}')$ over the bonds surrounding a unit cell of the lattice.

For an analytical approach it is essential that we consider an array which is either infinite or periodic, in both x and y directions. In fact, as we shall see later on, the single-junction solution (SJS) itself is not stable, and therefore irrelevant, for the finite array, where the junctions near the edges will behave differently from those in the bulk. These boundary effects do not have an important effect on measurements in a large system, but they seriously complicate a stability analysis. We therefore impose periodic boundaries, together with a current bias. This is nontrivial in itself, but can be achieved using the analysis presented in previous work.⁸ We apply the results of Ref. 8 to the staircase geometry, and remodel these time evolution equations to obtain a form which very much suits the present purpose. First we distinguish between bonds in the $\hat{x} + \hat{y}$ and $-\hat{x} + \hat{y}$ directions (see Fig. 1). We then write each bond variable appearing in Eq. (2.1) as a sum of three terms: a spatially homogeneous term, which is equal to the average over all bonds in the direction of the bond under consideration, a rotation-free and a divergence-free term. It is easy to see that, if we set both the sum of the homogeneous and the sum of the rotation-free terms in Eq. (2.1) equal to zero, then the sum of divergence-free terms vanishes automatically. We present the averages in the $\hat{x} + \hat{y}$ and $-\hat{x} + \hat{y}$ directions as $\Phi + \Psi$ and $\Phi - \Psi$, respectively, and altogether this gives us

$$\dot{\Phi}(t) = i_{\text{ext}}(t) - \frac{1}{N} \sum_{\mathbf{r}} \sum_{i=1,2} (\mathbf{a}_i \cdot \hat{y}) \sin[\phi(\mathbf{r}, \mathbf{r} + \mathbf{a}_i)], \quad (2.3a)$$

$$\dot{\Psi}(t) = -\frac{1}{N} \sum_{\mathbf{r}} \sum_{i=1,2} (\mathbf{a}_i \cdot \hat{x}) \sin[\phi(\mathbf{r}, \mathbf{r} + \mathbf{a}_i)], \quad (2.3b)$$

$$\dot{\varphi}(\mathbf{r}, t) = - \sum_{\mathbf{r}'} G(\mathbf{r} - \mathbf{r}') D(\mathbf{r}', t), \quad (2.3c)$$

with

$$D(\mathbf{r}, t) = \sum_{i=1}^4 \sin[\phi(\mathbf{r}, \mathbf{r} + \mathbf{a}_i)]. \quad (2.4)$$

Here $\phi(\mathbf{r}, \mathbf{r} + \mathbf{a}_i)$ is a shorthand notation for the total phase difference between \mathbf{r} and $\mathbf{r} + \mathbf{a}_i$:

$$\begin{aligned} \phi(\mathbf{r}, \mathbf{r} + \mathbf{a}_i) &= \Delta_{\mathbf{a}_i} \varphi(\mathbf{r}, t) + \varphi_0(\mathbf{r}, \mathbf{r} + \mathbf{a}_i) \\ &+ (\mathbf{a}_i \cdot \hat{\mathbf{y}})\Phi(t) + (\mathbf{a}_i \cdot \hat{\mathbf{x}})\Psi(t). \end{aligned} \quad (2.5)$$

The nearest neighbors \mathbf{a}_i are numbered $\mathbf{a}_1 = \hat{\mathbf{x}} + \hat{\mathbf{y}}$, $\mathbf{a}_2 = -\hat{\mathbf{x}} + \hat{\mathbf{y}}$, $\mathbf{a}_3 = -\hat{\mathbf{x}} - \hat{\mathbf{y}}$, $\mathbf{a}_4 = \hat{\mathbf{x}} - \hat{\mathbf{y}}$, and $\Delta_{\mathbf{a}_i} f(\mathbf{r}) = f(\mathbf{r}) - f(\mathbf{r} + \mathbf{a}_i)$. The magnetic field is incorporated through the ground-state configuration of gauge invariant phase differences, $\{\varphi_0(\mathbf{r}, \mathbf{r} ')\}$, which we assume to be known. The function G is the lattice Green's function in two dimensions, which can always be found by employing Fourier transform to invert the discrete Poisson equation

$$\sum_{i=1}^4 [G(\mathbf{r} + \mathbf{a}_i) - G(\mathbf{r})] = -\delta_{\mathbf{r}, \mathbf{0}}, \quad (2.6)$$

where δ represents the Kronecker function, as usual. Note that the current-biased periodic array can be seen as an array with periodic boundaries on the $\varphi(\mathbf{r}, t)$, but then together with time-dependent twists, $\Phi(t)$ and $\Psi(t)$, calculated per junction. These twists are determined in a self-consistent way, at every instant. The voltage difference, averaged over all junctions, is directly given by $\dot{\Phi}(t)$ in the y direction, and by $\dot{\Psi}(t)$ in the x direction.

Starting from Eqs. (2.3a)–(2.3c), we now derive the SJS and study its consequences in general. The phase differences in the ground state without an external current, $\varphi_0(\mathbf{r}, \mathbf{r} + \mathbf{a}_i)$, surely have to conserve supercurrents at every node \mathbf{r} . In fact, imposing conservation of supercurrents is equivalent to minimizing the total energy of the array. We can rephrase this conservation in terms of our quantities by saying that the $D(\mathbf{r}, t)$ are identically zero in the ground state, that is, they vanish if all $\varphi(\mathbf{r}, t)$ vanish together with $\Phi(t)$ and $\Psi(t)$. If we increase $i_{\text{ext}}(t)$ from zero, at $T = 0$, a simple reasoning shows that there is still a solution with all $D(\mathbf{r}, t)$ equal to zero if and only if, for all \mathbf{r} ,

$$\sum_{i=1}^4 (\mathbf{a}_i \cdot \hat{\mathbf{y}}) \cos[\varphi_0(\mathbf{r}, \mathbf{r} + \mathbf{a}_i)] = 0. \quad (2.7)$$

This condition is satisfied, in particular, if the $\varphi_0(\mathbf{r}, \mathbf{r} ')$ form a state which belongs to the class of staircase states introduced by Halsey,¹³ with the current injected in the direction of the staircases. These ground states appear, e.g., for $f = 0$, $\frac{1}{2}$, $\frac{1}{3}$, and $\frac{2}{5}$. The solution found here, with all $D(\mathbf{r}, t) \equiv 0$, is indeed a SJS because the voltage differences over all junctions in the array are identical.

Limiting ourselves to the staircase states, we have $\Psi(t) \equiv 0$ and the evolution equation for $\Phi(t)$ which follows from the SJS is

$$\dot{\Phi}(t) = i_{\text{ext}}(t) - C_f \sin[\Phi(t)], \quad (2.8)$$

with

$$C_f = \frac{1}{N} \sum_{\langle \mathbf{r}, \mathbf{r} ' \rangle} \cos[\varphi_0(\mathbf{r}, \mathbf{r} ')], \quad (2.9)$$

where the sum is over all junctions. We know that C_f is positive for all staircase states.¹³ Therefore we can transform Eq. (2.8) into a formal single-junction equation by rescaling the external current and the frequency. Still, we cannot simply use the single-junction results to determine the location and width of the steps. This is because the SJS is only relevant in practice when it is stable against small deviations. In the next section we therefore perform a stability analysis.

The simple SJS of Eq. (2.8) does not exist for arbitrary f , and in general the description is more complicated. In the cases considered by Sohn *et al.* and ourselves, the $i_{\text{dc}} - \langle v \rangle$ characteristic still does not show any $q > 1$ steps. So far, there is no understanding for these cases at the level of the individual junctions.

III. STABILITY ANALYSIS AND SIMULATIONS

In this section we study the stability of the SJS in arrays, using standard theory.¹⁶

We consider a staircase array, again current biased and with periodic boundaries, and we assume that f is such that the ground state of the system is a staircase state. We inject the external current, with $i_{\text{ac}} = 1.0$ and $\nu_0 = 0.1$, in the direction of the ground-state staircases in order to have an SJS. With Eq. (2.8) we can associate a single-junction situation, and we choose i_{dc} such that Eq. (2.8) has a stable τ_0 -periodic solution $\Phi_0(t)$. The important question now is whether the SJS is stable for the array. We write $\Phi(t) = \Phi_0(t) + \varepsilon(t)$ and linearize Eqs. (2.3a)–(2.3c) and (2.8), taking $\varepsilon(t)$ and all the $\varphi(\mathbf{r}, t)$ to be initially small. The equation for $\varepsilon(t)$ decouples from the rest of the set. We know beforehand that if we integrate this equation starting from $\varepsilon(0) = 1$ we get $|\lambda_\varepsilon| = |\varepsilon(\tau_0)| < 1$. This is because we arranged the τ_0 -periodic solution Φ_0 to be a stable solution of (2.8). For deviations in the array from single-junction behavior we therefore only consider the $\varphi(\mathbf{r}, t)$. The evolution equations for these deviations can be integrated numerically, starting with N initial conditions where only one $\varphi(\mathbf{r}, t = 0) = 1$ and all others are zero. The state vectors at time τ_0 are linearly combined to give eigenvectors, each with components $e_i(\mathbf{r})$, and we calculate the corresponding eigenvalues λ_i . According to the standard theory, the SJS is linearly stable, if $|\lambda_i| < 1$, for all $i = 1, \dots, N$.

The results for $|\lambda_i|$ are given in Fig. 2 for $f = \frac{1}{2}$ on a 4×4 lattice and for $f = \frac{1}{3}$ on a 3×3 lattice. For clarity we have discarded some eigenvalues for $f = \frac{1}{3}$ with magnitude much smaller than unity. We always have one state with eigenvalue unity, which corresponds to a global rotation of all phases. Because such a deviation does not have any physical consequences, we can safely ignore this eigenvalue in the stability analysis, and consequently we omitted this in Fig. 2. In the regions where the eigenvalues are drawn $|\lambda_\varepsilon| < 1$, and there the value of $\Phi_0(t)$ is on a Shapiro step. In the remaining regions (2.8) does not have a stable τ_0 -periodic solution. Figure 2 clearly shows that the SJS becomes unstable in the array before $|\lambda_\varepsilon| > 1$, i.e., before it becomes unstable for the single junction. Therefore the actual step width for the array is

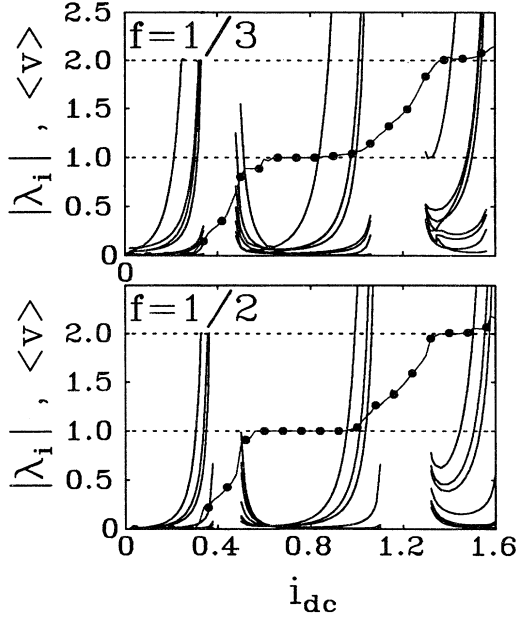


FIG. 2. Magnitude of the eigenvalues for $f = \frac{1}{2}$ and $f = \frac{1}{3}$ are plotted as solid lines. There is a Shapiro step for the single junction in the regions where eigenvalues are plotted, but for the array only in regions where all magnitudes of the eigenvalues are smaller than unity. We discard the eigenvalue unity, but we plot the dotted lines to locate the horizontal levels 1 and 2. The solid lines with the “•” are simulation results at very low temperatures. The small plateaus at noninteger values are an artifact of the boundary conditions.

smaller than found from a single-junction analysis based only upon Eq. (2.8). The step width also decreases much more rapidly with n [appearing below Eq. (1.1)] in the array, than for the SJS itself.

Suppose the array follows a SJS corresponding with $\langle v \rangle = 1$, and that $|\lambda_1| > 1$. If we disturb the situation by an amount $\varphi(\mathbf{r}, t = 0) = e_1(\mathbf{r})$, for all \mathbf{r} , then this will increase in amplitude with a constant factor, each period τ_0 , until the nonlinear effects take over. We usually observe that after several periods, each of which moves the vortex lattice over an integer multiple of the vector $2\hat{\mathbf{x}}$, there will be one period in which it moves over an additional vector $\hat{\mathbf{x}} \pm \hat{\mathbf{y}}$. After this, each new period τ_0 starts with this shifted vortex pattern. For this new situation the initial deviation e_1 always appears to be an eigenvector again, but now with $|\lambda| < 1$, so that it disappears. The resulting behavior of the array in the presence of a small noise source, is that there are periods where the vortex lattice shifts over an integer times $2\hat{\mathbf{x}}$, which randomly alternates with periods where it moves over an additional vector $\hat{\mathbf{x}} \pm \hat{\mathbf{y}}$.

On the basis of our present analysis we cannot be sure whether there are stable periodic solutions in case the SJS is an unstable solution. So far the simulations do not indicate this, but the behavior of arrays under these conditions is still under investigation.

To see the consequence of the instable modes for the $i_{dc} - \langle v \rangle$ curve, we simulated the periodic arrays, of the same sizes as in the stability analysis, using the al-

gorithm introduced previously.⁸ We update the phases using a second-order Runge-Kutta procedure with time steps of $0.05 \hbar / (2eI_c R_n)$. For each value of f we started our simulations from a ground-state configuration or from the final configuration of the previous i_{dc} . Each data point represents an average over several runs; in each run we average over 4000 configurations. At least 4000 configurations are discarded for large, initial relaxations and 1200 after small i_{dc} adjustments. For a substantial number of points we averaged over at least 40000 configurations after long relaxation times, and found no significant deviations from the results of the shorter runs. We take the temperature to be very small [$10^{-5} \hbar I_c / (2ek_B)$] but nonzero, in order to prevent the array from staying in unstable solutions. Our experience is that rounding errors by themselves are not always sufficient for this purpose. As usual, the effect of finite temperature is simulated by adding a white noise term to Eq. (2.1).

In Fig. 2 we added the results of simulations for $i_{ac} = 1.0$ and $\nu_0 = 0.1$, in several magnetic fields. We clearly see that $\langle v \rangle$ leaves a step when the largest eigenvalue becomes greater than unity. In a magnetic field the different eigenmodes become unstable at different values of i_{dc} , and as a consequence there is an intrinsic rounding of the curve, which is not caused by spatial inhomogeneities. Regions where $\langle v \rangle$ is a noninteger are characterized by an unstable SJS, and consequently the junctions voltages are nonsynchronous. Apart from minor deviations, the phase coupling to the rf source is retrieved when the SJS becomes stable again. We have verified that the solution is indeed of the SJS form on the steps. The largest magnitude of the eigenvalues appears to be exactly size independent in the periodic arrays, and consequently this also holds for the regions of phase locking, which correspond to this magnitude being smaller than unity. The reason for the lack of size dependence is that the corresponding eigenmode configuration has the same unit cell as the ground-state vortex pattern, and the periodic lattices always contain an integer number of these cells. In realistic arrays this size independence is expected as long as the system contains a large number of unit cells of the vortex lattice, which is usually the case. The small deviations between simulations and stability analysis generally arise when the largest $|\lambda_i|$ is just below unity. Here, our relatively short relaxation times do not allow the system to fall in the SJS. For $f = \frac{1}{3}$ there is an additional difference, due to the appearance of a (nearly) stable solution at $\langle v \rangle = \frac{2}{3}$. In this solution the staircases are oriented perpendicular to the current, and each period τ_0 they move over $2\hat{\mathbf{x}}$. If we decrease i_{dc} in small steps we do not see this because the SJS is also stable in that region. (Figure 2 represents an average over runs with increasing and decreasing i_{dc} , and therefore the small step lies in between $\frac{2}{3}$ and 1.) Simulations in a 6×6 periodic lattice and in the 8×8 finite lattice (discussed below) do not show the $\langle v \rangle = \frac{2}{3}$ step, and the other small steps at noninteger values for $f = \frac{1}{2}$, indicating that they are an artifact of the periodic boundary conditions.

In order to show that we can understand the behavior of realistic arrays with our analysis we also per-

formed simulations in a finite array of 8×8 unit cells (i.e., containing 256 junctions), again with temperature $10^{-5} \hbar I_c / (2ek_B)$. In Fig. 3 we give a set of $i_{dc} - \langle v \rangle$ curves both for finite and for periodic arrays. We confirm that there are only $q = 1$ steps present in these curves.¹⁴ The similarity between the two graphs in Fig. 3 indicates that the description of the periodic arrays also holds for the finite arrays. Nevertheless, the SJS itself is in general not a stable solution in the finite array, and the stable solution departs from full coherence near the edges. However, as a remainder of the SJS, there is still a solution with a homogeneous distribution of voltages near the center. Apparently, this counterpart of the SJS for the finite arrays is stable in about the same i_{dc} intervals where the SJS is stable in the periodic arrays. If we increase the size of the system, this solution will more and more resemble the homogeneous SJS. Note that in the finite arrays, apart from the intrinsic effect, the edges also add to the rounding of the curve near the steps, but this effect will be much smaller for the large arrays used in experiments.

The curves with $f \neq 0$ are almost mutually identical, with steps that are significantly smaller than for $f = 0$. Now, $C_{1/2} = 1/\sqrt{2}$ and $C_{1/3} = \frac{2}{3}$ do not differ very much, which means that the step widths on the basis of the SJS result are almost identical. From the stability analysis we

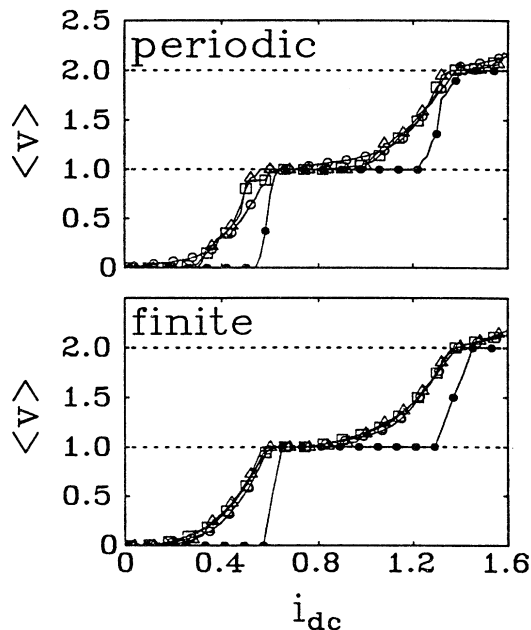


FIG. 3. The time-averaged voltage as a function of i_{dc} in periodic and finite (i.e., free-boundary) arrays. The magnetic fields are $f = 0$ (\bullet), $\frac{1}{2}$ (\triangle), $\frac{1}{3}$ (\square), $\frac{1}{4}$ (\circ), and for the finite arrays we also have $f = 1 - g$ ($*$), where $g = (\sqrt{5} - 1)/2$ is the golden mean. Only some of the data points are indicated by a marker. Again the dotted lines are plotted merely to define the exact locations of the integer levels.

see that, although the SJS is stable in a smaller region for $f = \frac{1}{3}$, the number of unstable eigenmodes is initially small. For this reason, the deviation from $\langle v \rangle = n$ is initially also small, which preserves the resemblance. As mentioned earlier, there is no clear comprehension of the data at the other values of f in Fig. 3.

IV. SUMMARY AND DISCUSSION

After rewriting the coupled set of evolution equations, describing the dynamics of the arrays, in a suitable form we construct a single-junction solution. We find the most general form of this coherent-phase solution together with the precise conditions which must be obeyed for it to appear. Subsequently the evolution equation is derived for the voltage difference over the array, in the case of a staircase ground state. A stability analysis shows that the array is phase locked to the rf source, i.e., that $\langle v \rangle$ is integer, in regions where the SJS is stable. Experiments on these arrays in a magnetic field will always show rounded steps. The reason for this intrinsic, field-dependent, rounding of the curve near the steps is that different modes become unstable at different i_{dc} . The results of this stability analysis can be particularly important for practical applications of the phenomenon.

We confirm that these arrays do not show the fractional Shapiro effect, i.e., the $q > 1$ steps. In simulations of periodic arrays we find that the system indeed follows the SJS in regions where the SJS is stable. These simulations also demonstrate the significance of the method, presented earlier,⁸ to simulate an array with periodic boundaries, in both x and y directions, together with a current bias.

As mentioned before, an earlier theoretical study of the staircase geometry led to subharmonics.¹⁵ The results of Ref. 14, as well as those presented here, do not confirm this. (Of course, the theoretical approach in question is based on a voltage bias, instead of a current bias, which obscures a direct comparison somewhat.) These subharmonics completely result from discontinuities in the twist $\alpha(t)$, in this work denoted by $\Phi(t)$, which are imposed through Eq. (12a) of Ref. 15 to describe the dynamics of the system when it enters a region in phase space where the SJS is unstable. Instead of imposing stability by forcing the system by hand to avoid these regions in phase space, we suggest simply letting the system, including the twist, evolve according to the coupled set of differential equations. Then, also with a voltage bias, one finds a SJS, and an analysis analogous to the one above should be employed to examine the stability of this solution.

When the ground state is not a staircase state, the SJS is no longer a solution. The $i_{dc} - \langle v \rangle$ characteristics are surprisingly similar to those of arrays with a staircase ground state, and we cannot fully understand this remarkable feature yet. Our conjecture is that the system will strive for a minimum spread of the voltages when it is phase locked. This is supported by preliminary simulations, which show that this spread decreases strongly on a step, although remaining nonzero.

Except for the consequences of unstable modes, we hardly tried to explain the results for this geometry us-

ing the vortex picture, which was successfully employed in case of the usual, straight, geometry. If we consider, e.g., the $\langle v \rangle = 1$ step, then the vortex lattice moves over its own unit cell in a time τ_0 , so that the starting and final configurations of each period are simple. However, the problem is that the intermediate configurations are generally quite complicated, and this prevents the vortex picture from giving additional insight.

ACKNOWLEDGMENTS

We thank P. Hadley for bringing Ref. 14 to our attention. This work was part of the research program of the Stichting voor Fundamenteel Onderzoek der Materie (FOM), which is financially supported by the Nederlandse Organisatie voor Wetenschappelijk Onderzoek (NWO).

-
- ¹S.P. Benz, M.S. Rzchowski, M. Tinkham, and C.J. Lobb, Phys. Rev. Lett. **64**, 693 (1990); Physica B **165&166**, 1645 (1990).
- ²K.H. Lee, D. Stroud, and J.S. Chung, Phys. Rev. Lett. **64**, 962 (1990).
- ³See, for example, M. Tinkham, *Introduction to Superconductivity* (McGraw-Hill, New York, 1975).
- ⁴J.U. Free, S.P. Benz, M.S. Rzchowski, M. Tinkham, C.J. Lobb, and M. Octavio, Phys. Rev. B **41**, 7267 (1990); S.P. Benz, J.U. Free, M.S. Rzchowski, M. Tinkham, C.J. Lobb, and M. Octavio, Physica B **165&166**, 1647 (1990).
- ⁵M.J. Renne and D. Polder, Rev. Phys. Appl. **9**, 25 (1974).
- ⁶R.L. Kautz, J.Appl.Phys. **52**, 3528 (1981).
- ⁷R.L. Kautz and R. Monaco, J.Appl.Phys. **57**, 875 (1985).
- ⁸H. Eikmans and J.E. van Himbergen, Phys. Rev. B **41**, 8927 (1990); H. Eikmans, J.E. van Himbergen, H.S.J. van der Zant, K. de Boer, and J.E. Mooij, Physica B **165&166**, 1569 (1990).
- ⁹H.S.J. van der Zant, H.A. Rijken, and J.E. Mooij, J. Low Temp. Phys. **82**, 67 (1991).
- ¹⁰M.S. Rzchowski, S.P. Benz, M. Tinkham, and C.J. Lobb, Phys. Rev. B. **42**, 2041 (1990).
- ¹¹S.P. Benz, M.S. Rzchowski, M. Tinkham, and C.J. Lobb, Phys. Rev. B **42**, 6165 (1990).
- ¹²S. Teitel and C. Jayaprakash, Phys. Rev. Lett. **51**, 1999 (1983).
- ¹³T.C. Halsey, Phys. Rev. B **31**, 5728 (1985).
- ¹⁴L.L. Sohn, M.S. Rzchowski, J.U. Free, S.P. Benz, M. Tinkham, and C. J. Lobb, Phys. Rev. B **44**, 925 (1991).
- ¹⁵T.C. Halsey, Phys. Rev. B **41**, 11 634 (1990).
- ¹⁶See, for example, J.G. Malkin, *Theorie der Stabilität einer Bewegung* (Oldenbourg, München, Germany, 1959).